

THREE PRACTICAL EXAMPLES OF MAGNETIC BEARING CONTROL DESIGN USING A MODERN TOOL

M. Spirig and J. Schmied
Delta JS AG, Switzerland

P. Jenckel and U. Kanne
LUST Antriebstechnik, Germany

ABSTRACT

The use of magnetic bearing in industrial applications has increased due to their unique properties. Nowadays efficiency and predictability in handling rotors on magnetic bearings is asked with the same standard as conventional rotors on oil or roller bearings.

First of all one must be aware of the special technical properties of magnetic bearing designs. The dynamic behaviour of the rotor combined with requirements of the application define the desired bearing characteristic. With modern tools [1], covering the mechanical aspects as well as the electronic controllers and their digital implementation on a DSP, these properties can be designed.

However, despite the use of such efficient tools engineering practice is needed. Therefore this paper summarises the major steps in the control design process of industrial applications. Three rotors supported on magnetic bearing with their specific dynamic behaviour are presented:

- A very small high speed spindle (120000 rpm),
 - a small, industrial turbo molecular pump rotor (36000 rpm) and
 - a large multi-stage centrifugal compressor (600 to 6300 rpm).
- The results of the analyses and their experimental verification are given.

1. INTRODUCTION

1.1 Technical considerations in magnetic bearing design

The allowable rotor vibrations in magnetic bearing applications are limited e.g. due to small clearances, bearing capacity limits, limited driving torque when crossing critical speeds etc. and therefore have to be specified. Design specifications for the rotor damping and the location of critical speeds, such as API 617, can be used as guidelines. However, they do not cover all aspects. Basic questions in the case of any rotating machine design are [1]:

- Where are the critical speeds? Are critical speeds within the operating speed range? How many critical speeds must be crossed during the run up of the rotor?
- What is the necessary damping of the natural modes of the rotor in order to ensure safe run up and operation? How can it be achieved?
- What is the necessary stiffness of the bearing? How can it be achieved?

These questions have higher significance in the magnetic bearing design, especially because of the limited specific bearing capacity. At low frequencies the capacity is around 0.3 - 1 MPa, because of the magnetic saturation of the material. It is even further reduced at higher frequencies due to the limited voltage of the power amplifiers [2],[7]. Excessive bearing loads lead to a contact of the rotor with the auxiliary bearings. Normally they are ball bearings or bushings with a low friction surface. Each contact wears them out more and more. That is why loads, which can occur during a rotor lifetime have to be considered very carefully in the design process.

An optimal damping is mandatory for any robust rotor design. In most applications the damping has to be provided by the bearing. In order to enable a magnetic bearing to do this, all natural modes, which must be well damped (normally all modes below the maximum operating speed), must be observable and controllable. Sufficient damping force must be provided by a controller design, which yields the appropriate amplitude and phase angle of the bearing transfer function. A damping characteristic is achieved for phase angles $0^\circ < \phi < 90^\circ$ or $-180^\circ > \phi > -270^\circ$ (see fig. 1, 3 and 6).

In some applications a sufficient stiffness force is also important e.g. to resist high fluid forces, which normally have very low frequencies. With speed the behaviour of a rotor may change due to gyroscopic effects or due to changes in the fluid forces. A robust controller design as presented in section 2 for the three different rotors must take all this into account.

1.2 Tools for the rotordynamic analyses

Software tools suited for the engineering of magnetic bearing applications must comprise a structural part describing the rotor (/3/, /4/, /5/) as well as a mechatronic part describing the magnetic bearing and the combined rotor bearing system. A relatively simple practical way of looking at the combined system is described in /9/. The necessary software capabilities are listed in the following.

- The structural part has to consider:
 - Gyroscopic effects,
 - rotor fluid interaction, such as labyrinth induced excitations,
 - dynamics of flexible parts mounted on the rotor, such as disks,
 - flexibility of stator parts.
- The mechatronic part has to consider:
 - Non-collocation of sensors and actuators,
 - magnetic pull (negative stiffness) of magnetic actuators,
 - digital controllers, taking into account the antialiasing filter, a time delay and the AD conversion,
 - characteristics of the hardware components of magnetic bearings (sensors and amplifiers),
 - separate sensors as well as separate controllers for displacement and velocity,
 - coupling of bearings and / or axes by means of controllers e.g. different controllers for tilting and translation rotor modes.

A comprehensive tool is illustrated in /1/ and /8/. It also includes a controller design part, which allows to create the transfer function with the required amplitude and phase by combining standard controller components e.g. modified PID controllers (see appendix), first and second order filters, all pass, notch and analogue Butterworth filters.

1.3 Typical engineering procedure

The major steps in the control design process are:

- Modelling the structural part in a similar way as in case of conventional bearings (see table 1 and 2 in the appendix).
- Studying the basic behaviour of the rotor, including the analyses of natural frequencies of the rotor at standstill and at speed for different bearing stiffness coefficients, as well as the analyses of the damping ratios (see appendix) of natural modes for different bearing damping coefficients.
- Define the requirements and / or determine the properties of the electronic hardware and software as listed in section 1.2.
- Design of the controller transfer function /7/, taking into account the basic behaviour of the rotor as well as the requirements of the application (section 2).
- Study the actual behaviour of the combined system in a closed loop analysis (/1/, section 3).

This procedure is demonstrated in detail for three applications in the next sections.

2. ROTORS, APPLICATIONS REQUIREMENTS AND CONTROLLERS

The first step in the design procedure is to model the rotor structure and study its basic behaviour /4/. The main data of the three very different rotors are summarised in table 1 in the appendix. Table 2 in the appendix shows the dimensions, the mass

and stiffness diameters, the locations of the supports (triangles) and the arrangement of the nodes. Also the concentrated masses and the flexible disk of the third rotor are visible.

The lower part of table 2 in the appendix shows the mode shapes of the free rotors at standstill, which will be important in the later controller design. The long vertical lines indicate the actuator locations and the shorter vertical lines the sensor locations. The natural frequencies and the range of the frequencies as the rotor starts rotating up to its maximum speed are listed above the mode shapes.

2.1 Rotor 1: Small high speed rotor

The first rotor is a very small spindle realised in a research project /1/. It rotates supercritically at the very high speed of 120000 rpm = 2000 cps.

- Basic behaviour of the rotor (table 2 in the appendix)
The natural frequency of the free rotor's first bending mode is at 1714 Hz. In order to cross this mode considerable damping forces have to be provided by the bearings at an extremely high frequency.

- The electronic hard- and software
Digital hardware is used to implement the controller. Due to the high frequency range of this small rotor the phase losses of the electronic components are quite important (fig. 1, B). At 1714 Hz they consist of the following components.

- The time delay is one period of the sampling rate, i.e. it is 96µs, which corresponds to 59°. Within this time the A/D conversion as well as the signal processing takes place.
- The zero order hold behaviour /6/ of the digital controller with a sampling rate of 10400 Hz adds another 30°.
- The amplifier i.e. the current controller has more than 45°.

The magnetic bearings each have a negative stiffness of about 53000 N/m. The motor also has a negative stiffness in the same order of magnitude. Hence the stiffness of the bearings created by the controller should be at least around 2-3 10⁵ N/m in order to safely compensate these negative stiffnesses.

- Design of the controller
Due to the above mentioned phase losses it is impossible to damp the first bending mode with a phase angle above 0°. This could only be achieved by a phase angle below -180°. The transfer function of the bearings is shown in fig. 1. Both bearings have the same function. The figure contains several curves, which demonstrate the influence of various effects.

1 Controller with its analogue transfer function digitally transformed by the "first order hold" (foh, /6/) method. This is how it is programmed in the processor. The foh method gives a good approximation to the analogue transfer function. The amplifier characteristic is also included and foh transformed as well. The curve is composed of the following elements:

- A modified PID element (see the "base" function in the appendix) to damp the rigid body modes by phase lead (A).
- A second order filter at 1100 Hz to lower the phase below -180° in order to damp the first bending mode at 1714 Hz (C).
- A second order filter at 2200 Hz approximating the amplifier.

- 2 The controller and amplifier in their analogue form including an analogue antialiasing filter of first order at the frequency of 5200 Hz. This filter has almost no influence in the frequency range up to 2000 Hz.
 - 3 The analogue form of the controller, amplifier and antialiasing filter (curve 2) plus the time delay of 96 μs , which lowers the phase angle significantly.
 - 4 Curve 3 digitally transformed by the “zero order hold” (zoh, /6) method. The transfer function including the zoh behaviour gives an additional phase loss.
- Curve 2 to 4 are only plotted for design purposes of the controller, to show the phase losses (fig. 1, B). The actual closed loop model is built by the digital bearing transfer function transformed by first order hold (thick solid curve 1) combined with the zoh transformed model of the rotor with the analogue antialiasing filter switched in series.

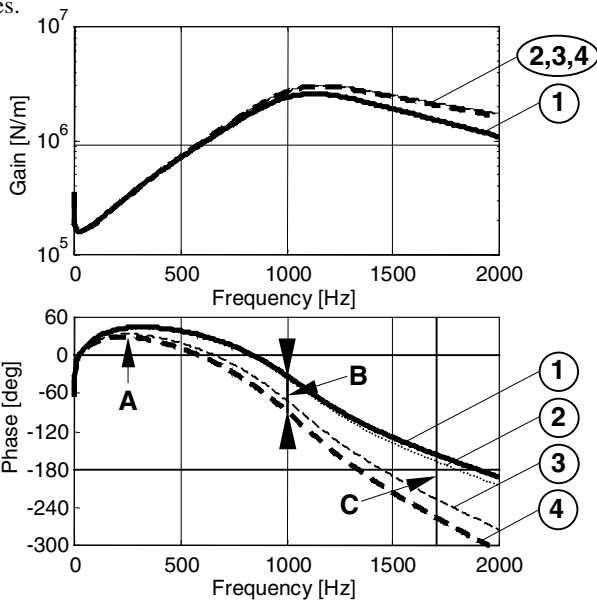


Fig. 1 Bearing Transfer Function of the High Speed Rotor

2.2 Rotor 2: Industrial turbo molecular pump (TMP)

The second rotor is an industrial turbo molecular pump. It runs at a maximum speed of 36000 rpm.

- Basic behaviour of the rotor (table 2 in the appendix)
- Due to the shape including the large disks with blades the ratio of the polar moment of inertia to the transverse moment of inertia is quite high (see table 1 in the appendix). Therefore the gyroscopic effect is quite extreme, as can be seen in fig. 2. The forward tilting mode frequency rises with the speed from 0 to 250 Hz. Beside the rotor modes, blade modes between 600 and 800 Hz play a role, although they are not coupled with rotor modes to a high extent. However, in the testing phase it turned out, that they had to be considered in the controller design. In the theoretical model they are assumed as rigid. The first elastic rotor mode is at a frequency of 1200 Hz.

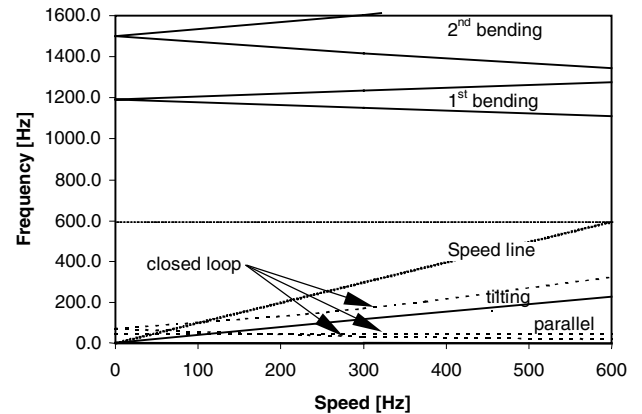


Fig. 2 Natural Frequencies of the Modes vs. Speed for the Free and Supported Rotor

- The electronic hard- and software
- Also in this application the phase losses of the electronic components i.e. of the amplifier, the antialiasing filter of second order at 4450 Hz, the time delay of 64 μs and of the digital controller sampling rate of 8900 Hz cannot be neglected. The magnetic pull of the bearing in this case is $2.4 \cdot 10^5 \text{ N/m}$ for the upper bearing (left in table 2 in the appendix) and $3.0 \cdot 10^5 \text{ N/m}$ for the lower bearing (right in table 2 in the appendix)

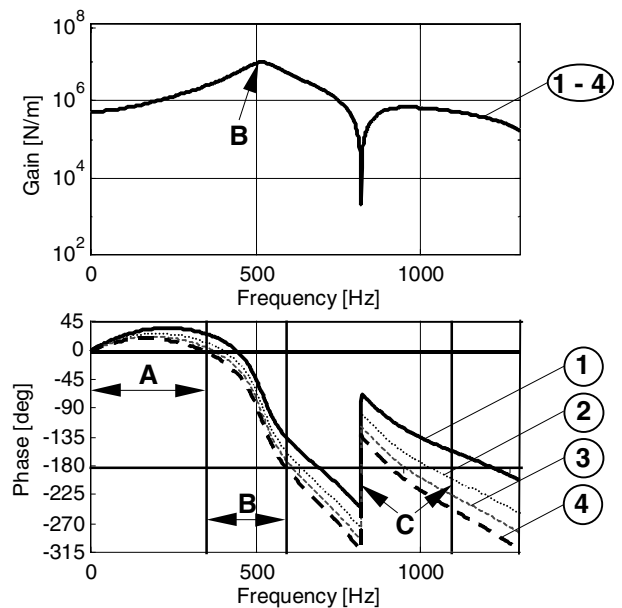


Fig. 3 Bearing Transfer Function of the TMP

- Design of the controller
- The transfer function of the bearings is shown in fig. 3 in the same way as in fig. 1. The basic design ideas are:
- A The range with positive phase is enlarged up to 330 Hz, in order to damp the widely spread tilting modes. This is done with a phase lead part of a PID element at 170 Hz (see the "base" function in the appendix).

B In order to provide damping at the frequency of the blade modes the phase has to be dropped rapidly below -180° . This is achieved by a second order element in the denominator (phase lag element in the "base" function in the appendix), which has a frequency of 520 Hz. This has also the effect of reducing the amplitude

C In order to provide damping for the rotor mode at 1200 Hz the fast phase loss, which would drop even below -360° is interrupted by a notch filter at 820 Hz.

2.3 Rotor 3: Large industrial centrifugal compressor

The third rotor is a large industrial multi-stage centrifugal compressor [8]. It is driven by a 23 MW variable speed synchronous electric motor, with a wide operating speed range from 600 rpm to 6300 rpm.

- Basic behaviour of the rotor (table 2 in the appendix)

At low frequencies the rotor is exposed to considerable fluid forces. The first bending mode is at 64 Hz. Hence it is in the operating speed range and requires special attention. The frequency of the one nodal diameter vibration mode of the axial bearing disk is at 490 Hz. It had to be considered in the model for the controller design, since it strongly interacts with rotor modes. In the second and higher bending modes the flexible disk tilts more than a rigid disk would (see the mode shapes in table 2 in the appendix). This has the effect of considerably increasing the gyroscopic effect. In fig. 4 and 5 the natural frequencies are presented as a function of the bearing stiffness at different speeds for a rigid and a flexible disk. The comparison of both results show, that the frequency difference between forward and backward whirl as well as the frequency regions where the bearing has to provide damping increase considerably in case of the flexible disk.

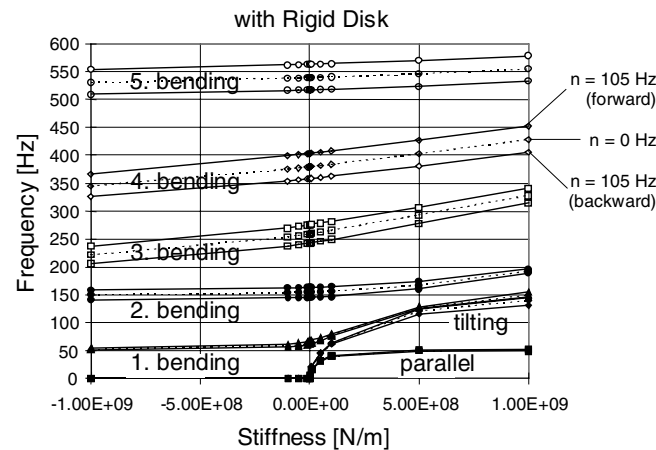


Fig. 4 Natural Frequencies of the Modes vs. Bearing Stiffness and Speed (rigid fixed disk)

- The electronic hard- and software

As in the previous cases, the controller is implemented on a digital system with a sampling rate of 10000 Hz. The phase losses due to the digitalisation and the hardware are considered, however, in this case they are not as important as in the previous cases, due to the lower frequencies.

The magnetic pull of the actuator, which has to be compensated by the controller, has a value of $1.57 \cdot 10^7$ N/m.

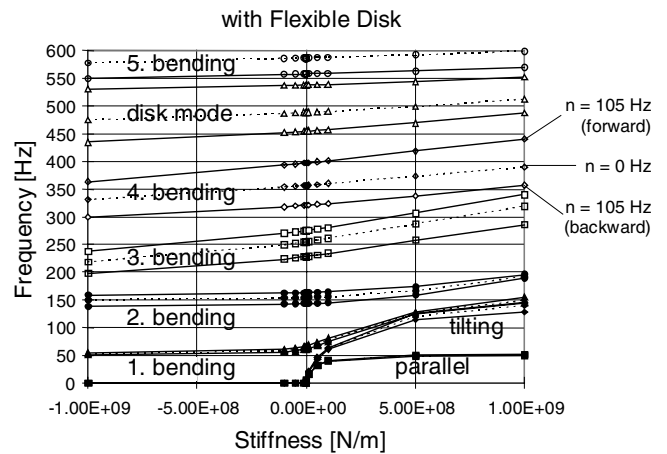


Fig. 5 Natural Frequencies of the Modes vs. Bearing Stiffness and Speed (flexible fixed disk)

- Design of the controller

Figure 6 shows the magnetic bearing transfer function including the sensor, the antialiasing filter, the controller, the amplifier the actuator and the time delay.

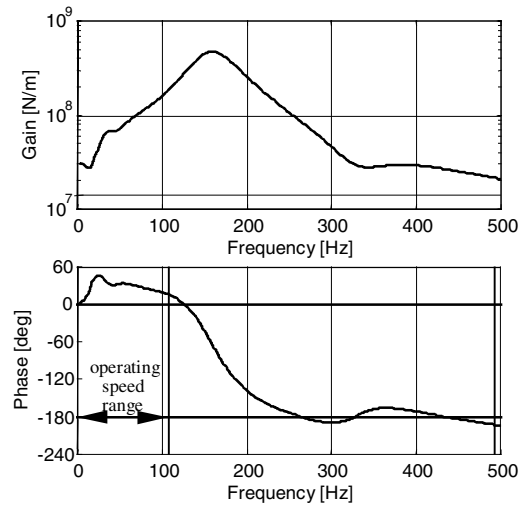


Fig. 6 Bearing Transfer Function of the Large Industrial Centrifugal Compressor

Important features of the controller are:

- To resist the high fluid forces at low frequencies the stiffness has to be above a certain limit.
- In order to damp the rigid body modes, which are mostly affected by the destabilising labyrinth seal forces, the phase is increased by an extra filter at 18 Hz.
- To prevent saturation of the amplifier the amplitudes at high frequencies are reduced with a second order low pass filter. The phase decreases below 0° , which yields a negative damping force for the second bending mode. However, this mode has a node slightly inside the outboard sensor. The deflections at the sensor

and the actuator have reverse sign and thus the mode is slightly damped. At higher frequencies the bearing provides a damping force thanks to the phase angle below -180° .

The overall controller transfer function is an eighteenth order polynomial. It is designed by the bearing manufacturer using his own controller design software. To fully optimise the controller for this application the transfer function is synthesised with complex rather than simple poles and zeros. Digital controller hardware is essential to the implementation of this type of controller transfer function.

3 CLOSED LOOP BEHAVIOUR

Once a controller is designed considering the basic rotor behaviour and the application requirements, the actual behaviour of the combined system can be studied. The comparison between analysis and measurements can bring up possible deficiencies of the model. Often this helps to complete the model and thus improves iteratively the prediction and the behaviour of the final closed loop system. The degree of agreement between reality and prediction depends mainly on the complexity of the rotor e.g. shrunk parts, elasticity of parts mounted on the rotor, etc. and how accurate it can be modelled. A fine tuning after implementation of the controller may be necessary.

In the following sections the calculated closed loop behaviour and the experimental verification of the analysis are presented for the three rotors:

- First the calculated eigenvalues composed of the natural frequency (+ forward, - backward whirling) and the damping ratio of the combined rotor bearing system at standstill and nominal speed are listed for each case. The tables (3 - 5) contain the eigenvalues, which can be assigned to the rotor. Besides that some eigenvalues are caused by controller poles, which interact with the rotor. This interaction can change their frequency and damping ratio. The eigenvalues caused by the controller with a damping ratio below 20% are also shown in the tables.
- Second examples of the calculated and measured responses to force or unbalance excitation are given.

3.1 Rotor 1: High speed rotor

Table 3: Natural Frequencies and Damping Ratios

Speed	n = 0 [Hz]		n = 2000 [Hz]	
	Frequency [Hz]	Damping Ratio [%]	Frequency [Hz]	Damping Ratio [%]
parallel	89.7	29.5	- 88.7	29.7
			+ 89.9	29.6
tilting	145.9	49.7	- 100.1	45.8
			+ 229.5	43.6
1 st bending	1709.6	3.9	- 1534.4	4.1
			+1787.5	2.5
2 nd bending	4856.2	0.6	- 4635.4	0.7
			+ 5069.7	0.6

In table 3 can be seen that the rigid modes are well damped. The first forward whirling bending mode at speed has a damping

ratio of only 2.5 %. This has to be improved, among others by a higher gain. The higher gain can only be realised with a balance compensation system as the tests showed. At this moment such a system is being optimised. A speed of 1600 Hz has been reached.

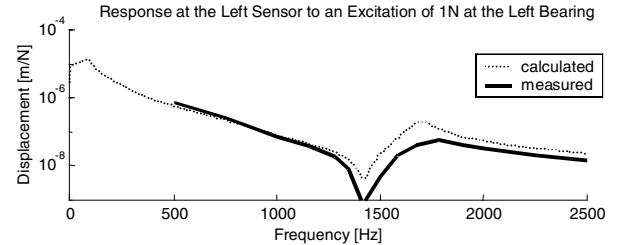


Fig. 7 Measured and Calculated Responses at Standstill

The closed loop behaviour at standstill is confirmed by comparison of calculated and measured transfer functions with an excitation by the bearing. Figure 7 shows the response at the left sensor location to an excitation of 1 N at the left bearing. The resonance of the rotor's first bending at 1709 Hz as well as the frequency of the anti resonance agree well.

The damping of the bending mode $\approx 6\%$ is higher in the measurement. Possible reasons for this are the inner damping of the rotor and the external damping of the surrounding air.

3.2 Rotor 2, small industrial turbo molecular pump

Table 4: Natural Frequencies and Damping Ratios

Speed	n = 0 [Hz]		n = 600 [Hz]	
	Frequency [Hz]	Damping Ratio [%]	Frequency [Hz]	Damping Ratio [%]
parallel	38.7	17.0	- 38.4	16.8
			+ 38.5	16.9
tilting	70.2	24.7	- 13.5	9.5
			+ 296.8	9.7
contr. pole 520, 10	481.2	12.4	- 431.9	16.6
			+ 495.1	11.5
contr. pole 520, 10	512.0	11.0	- 511.2	11.1
			+ 513.0	11.0
contr. pole 820, 17	801.6	16.9	- 799.0	16.9
			+ 803.5	17.0
contr. pole 820, 17	809.9	17.7	- 809.6	17.6
			+ 810.0	17.7
1 st bending	1193.3	0.3	- 1107.7	0.4
			+ 1274.1	0.3
contr. pole 1400, 18.6	1373.1	18.8	- 1372.7	18.8
			+ 1373.4	18.7
contr. pole 1400, 18.6	1374.9	18.6	- 1374.7	18.6
			+ 1375.1	18.6
2 nd bending	1501.0	0.2	- 1344.3	0.3
			+ 1724.4	0.1

The modes within the speed range shown in table 4 are well damped. The higher modes are stable with low damping ratios.

For this rotor the behaviour is confirmed by a comparison of a calculated and measured transfer function.

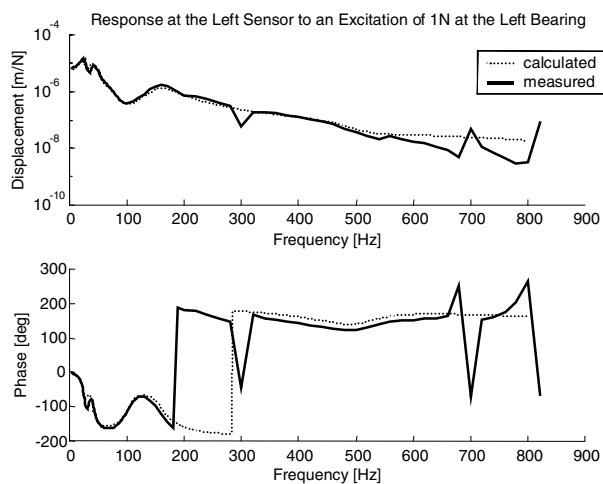


Fig. 8 Measured and Calculated Responses at 300 cps

Figure 8 shows a good agreement of the responses at the left sensor location to an excitation of 1N at the left bearing. The resonances of the tilting mode as well as of the parallel mode are well visible. In addition, the measurement at 300 Hz shows the influence of the unbalance, which is not included in the load case of the calculation. In the region of 700 to 800 Hz the calculated curve deviates from the measured curve. This is probably due to elastic blade modes, which are not considered in the model.

3.3 Rotor 3: Large industrial centrifugal compressor

Table 5: Natural Frequencies and Damping Ratios

Speed	n = 0 [Hz]		n = 105 [Hz]	
	Frequency [Hz]	Damping Ratio [%]	Frequency [Hz]	Damping Ratio [%]
parallel	12.6	25.8	-12.6 +12.6	25.8
tilting	14.0	28.8	- 13.8 + 14.1	28.8 28.9
contr. pole 35.8, 40	35.8	18.5	- 35.7 + 35.9	18.3 18.7
1 st bending	81.2	19.8	- 77.3 + 84.7	21.0 19.2
contr. pole 161, 20	130	6.8	- 129 + 131	7.8 6.5
contr. pole 161, 20	131	9.5	- 131 + 132	12.3 15.5
2 nd bending	155	1.4	- 143 + 164	1.5 1
3 rd bending	250	0	- 223 + 272	0 0
4 th bending	355	0	- 320 + 396	0 0
Rotor disk mode	488	0	- 454 + 538	0 0
4 th bending	587	0	- 558 + 631	0 0

In table 5 all damping ratios of the modes below the maximum speed are very well damped. The first bending mode, which is within the operating speed range, has a damping ratio of 20%. This complies with the specification according to API 617 for compressors, although its application to compressors supported on magnetic bearings is controversial.

Figure 9 shows the calculated and measured bearing response of the right bearing to an unbalance magnitude of G2, i.e. 3300 gmm are applied at the thrust disk and 2700 gmm at the coupling. This distribution yields a good excitation for the first bending mode. The maximum force below the maximum speed of 6300 rpm remains below the dynamic capacity of 20000 N peak-peak.

The agreement between measurement and calculation is good. The calculated force at higher speeds, where the compressor never runs, increases due to the controller dominated pole at 130 Hz, which has a relatively low damping. Also the measured force remains at a high level up to maximum speed for the same reason.

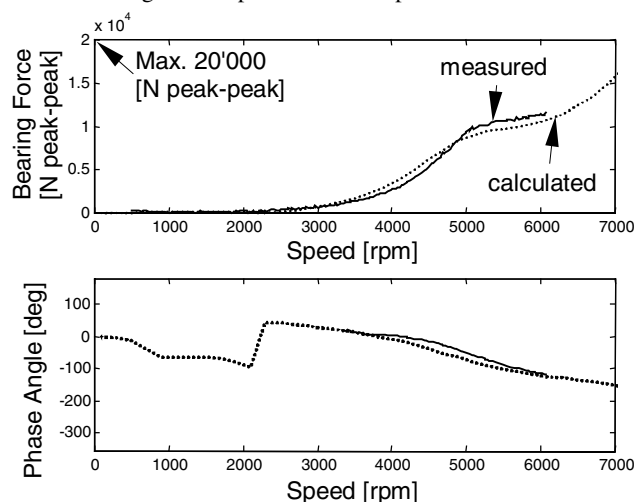


Fig. 9 DE Bearing Response to an Unbalance G2 (peak-peak amplitude)

4 CONCLUSIONS

Efficiency and predictability in handling rotors on magnetic bearings is achieved by using a modern design tool (/1/ and /8/). The typical design procedure is presented. Its main steps are:

- The study of the mechanical part i.e. modelling the rotor structure and investigate it's basic behaviour.
- The study of the mechatronic part i.e. defining the requirements or determining the properties of the electronic hard- and software.
- The design of the controller i.e. generating the bearing transfer function considering the gain as well as the phase.
- The study and interpretation of the closed loop behaviour.

This procedure is iterative and needs engineering practice. Therefore the paper presents three applications.

- A very small high speed spindle running at a maximum speed of 120000 rpm, which is above the natural frequency of the free rotor's first bending mode at 1714 Hz. Because of this high speed, the phase losses of the electronic components and of the digitizing process are of special importance.

- A small, industrial turbo molecular pump rotor running at a maximum speed of 36000 rpm. Due to its shape this rotor has a pronounced gyroscopic effect. For this reason the frequency range between the forward and backward tilting mode is widely spread from 0 to 320 Hz. Above that, elastic blade modes in the region of 600 to 800 Hz had to be considered for the controller design.
- A large industrial multi-stage centrifugal compressor with an operating speed range from 600 rpm to 6300 rpm. This rotor is subject to high fluid forces at low frequency, has its first bending mode within the operating speed and has a flexible axial bearing disk, which strongly interacts with the rotor modes and which played an important role for the controller design.

The result of the design process is the transfer function of the bearing controller and the prediction of the closed loop behaviour. The extent of predictability depends on the complexity of the rotor and how accurate it can be modelled. The accuracy also depends on tolerances, which play an important role, especially in case of the small rotors. However, a model always helps to accelerate and improve the design, even for cases where the theoretical model is not a complete representation of the reality. In some cases the final implementation of the controller may require a fine tuning.

For all three presented rotors a comparison of calculation and measurement has been carried out. The result can be summarised as follows:

- For the high speed spindle the measured performance of the bearing is better than predicted. The higher damping ratio of the first bending mode is probably due to damping effects, which are not part of the model.
- For the turbomolecular pump good agreement is achieved apart from elastic blade modes, which were not considered. They are rigidly modelled, since they did not seem to interact with the rotor. In this regard the model turned out to be insufficient.
- For the industrial turbocompressor the theoretical prediction is very good, after the elasticity of the axial bearing disk has been taken into account.

ACKNOWLEDGEMENTS

The authors wish to thank the Swiss Federal Institute of Technology ETH and Sulzer Electronics for their co-operation in the high speed spindle research project. We also thank Federal Mogul Magnetic Bearings and Demag Delaval for their support concerning the industrial turbo compressor project. Special thanks to Frits de Jongh for the excellent co-ordination during the project and for the unbalance response measurements.

REFERENCES

- /1/ J. Schmied, F. Betschon, 1998, "Engineering for Rotors Supported on Magnetic Bearings", Proceedings of the 6th International Symposium on Magnetic Bearings, Boston.
- /2/ E. Maslen et al., April 1989, "Practical Limits to the Performance of Magnetic Bearings: Peak Force, Slew Rate, and Displacement Sensitivity", ASME Journal of Tribology.
- /3/ J. W. Lund, May 1974, "Stability and Damped Critical Speeds of a Flexible Rotor in Fluid-Film Bearings", Journal of Engineering for Industry.
- /4/ H. D. Klement, 1993, "Berechnung der Eigenfrequenz und Stabilität von Rotoren mit MADYN", VDI Bericht Nr. 1082.
- /5/ H. D. Nelson, J.M. Vaugh, May 1976, "The Dynamics of Rotor-Bearing Systems Using Finite Elements", Journal of Engineering for Industry.
- /6/ /x/ G. F. Franklin, J. D. Powell, M. L. Workman, 1994, "Digital Control of Dynamic Systems", Second Edition, Addison-Wesley Publishing Company, Inc., New York.
- /7/ Proceedings of MAG '97, Session 6 & 7, 1997, "Industrial Conference and Exhibition on Magnetic Bearings", University of Virginia, Technomic, Lancaster, PA.
- /8/ J. Schmied, A.B.M. Nijhuis, R. R. Shultz, 1999, "Rotordynamic Design Considerations for the 23MW NAM-GLT Compressor with Magnetic Bearings", IMechE Fluid Machinery Symposium, The Hague.
- /9/ K. A. Schoeneck, J. F. Hustak, 1987, "Comparison of Analytical and Field Experience for a Centrifugal Compressor Using Active Magnetic Bearings", IMechE C104/87.

APPENDIX

Definition of the Damping Ratio

$$D = \frac{\text{Re}(Eigenvalue)}{|Eigenvalue|} \approx \frac{\log. Decrement}{2 \cdot \pi} \approx \frac{1}{2 \cdot Ampl. Factor}$$

Base Function (MEDYN Function "base" /1/)

The base function is a modified PID-controller. The function has the following structure:

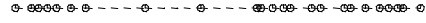
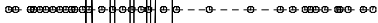
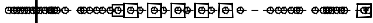
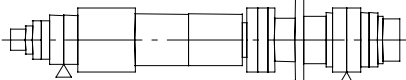
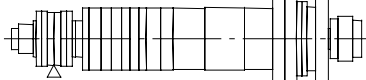
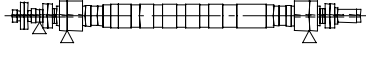
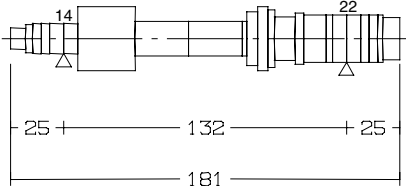
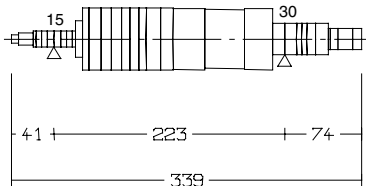
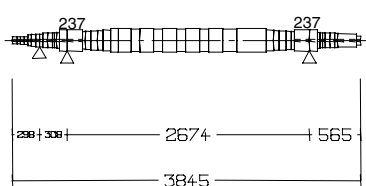
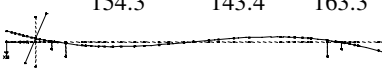
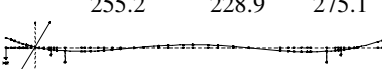
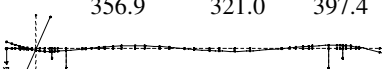
$$F_{base} = \frac{(P_{n1} + \frac{(P_{n1} + P)s}{2\pi f_{n1}})(1 + \frac{s}{2\pi f_{n2}})}{(1 + \frac{s}{2\pi f_{d1}})(1 + \frac{s}{2\pi f_{d2}})} + \frac{(P_{n1} + P)2\pi f_{in}}{s} + P$$

phase lead / lag 1 phase lead / lag 2 integrator P-part

Table 1: Summary of the Main Rotor Data

	High Speed Spindle		Turbo Molecular Pump		Centrifugal Compressor	
Mass	0.68	kg	6.3	kg	2.1 10 ³	kg
Polar Moment of Inertia	6.2 10 ⁻⁵	kgm ²	1.6 10 ⁻²	kgm ²	4.1 10 ¹	kgm ²
Diametral Moment of Inertia	1.5 10 ⁻³	kgm ²	4.0 10 ⁻²	kgm ²	2.2 10 ³	kgm ²
Rotor Diameter (Bearing)	14 / 22	mm	15 / 30	mm	237	mm
Rotor Length	181	mm	344	mm	3845	mm
Bearing Span	132	mm	223	mm	2674	mm
Max. continuous speed	120000	rpm	36000	rpm	6300	rpm

Table 2: Rotor Models, Mode Shapes and Natural Frequencies

High Speed Spindle	Turbo Molecular Pump	Centrifugal Compressor																		
																				
NODS / CONCENTRATED MASSES	NODS / CONCENTRATED MASSES	NODS / DISK / CONCENTRATED MASSES																		
																				
MASS DIAMETER	MASS DIAMETER	MASS DIAMETER																		
																				
DIMENSIONS / STIFFNESS DIAMETER	DIMENSIONS / STIFFNESS DIAMETER	DIMENSIONS / STIFFNESS DIAMETER																		
Mode Shapes (at standstill) and Natural Frequencies of the Free Rotors (Hz)																				
<table border="0"> <tr> <td>Standstill</td> <td colspan="2">n = 2000 Hz</td> </tr> <tr> <td></td> <td>backward</td> <td>forward</td> </tr> </table>	Standstill	n = 2000 Hz			backward	forward	<table border="0"> <tr> <td>Standstill</td> <td colspan="2">n = 600 Hz</td> </tr> <tr> <td></td> <td>backward</td> <td>forward</td> </tr> </table>	Standstill	n = 600 Hz			backward	forward	<table border="0"> <tr> <td>Standstill</td> <td colspan="2">n = 105 Hz</td> </tr> <tr> <td></td> <td>backward</td> <td>forward</td> </tr> </table>	Standstill	n = 105 Hz			backward	forward
Standstill	n = 2000 Hz																			
	backward	forward																		
Standstill	n = 600 Hz																			
	backward	forward																		
Standstill	n = 105 Hz																			
	backward	forward																		
<u>parallel</u>	<u>parallel</u>	<u>1. bending</u>																		
0.0 0.0 0.0	0.0 0.0 0.0	64.3 61.4 67.2																		
																				
<u>tilting</u>	<u>tilting</u>	<u>2. bending</u>																		
0.0 0.0 77.4	0.0 0.0 228.8	154.3 143.4 163.3																		
																				
<u>1. bending</u>	<u>1. bending</u>	<u>3. bending</u>																		
1714.3 1582.9 1856.0	1195.7 1110.7 1275.9	255.2 228.9 275.1																		
																				
<u>2. bending</u>	<u>2. bending</u>	<u>4. bending</u>																		
5543.9 5330.3 5764.7	1501.7 1344.8 1724.5	356.9 321.0 397.4																		
																				
<u>3. bending</u>	<u>3. bending</u>	<u>disk mode</u>																		
10281.9 9979.9 10588.0	2641.4 2446.8 2851.4	488.1 454.8 538.1																		
